Journal of Zhejiang University-SCIENCE A (Applied Physics & Engineering)
ISSN 1673-565X (Print); ISSN 1862-1775 (Online)
www.zju.edu.cn/jzus; www.springerlink.com
E-mail: jzus@zju.edu.cn

Prediction of extreme wind velocity at the site of the Runyang Suspension Bridge*

Yang DENG†, You-liang DING†‡, Ai-qun LI, Guang-dong ZHOU

(*Key Laboratory of Concrete and Prestressed Concrete Structures of Ministry of Education, Southeast University, Nanjing 210096, China*)

†E-mail: seudengyang@yahoo.com.cn; civilding@163.com

Received Oct. 28, 2010; Revision accepted May 15, 2011; Crosschecked July 4, 2011

Abstract: This paper presents a distribution free method for predicting the extreme wind velocity from wind monitoring data at the site of the Runyang Suspension Bridge (RSB), China using the maximum entropy theory. The maximum entropy theory is a rational approach for choosing the most unbiased probability distribution from a small sample, which is consistent with available data and contains a minimum of spurious information. In this paper, the theory is used for estimating a joint probability density function considering the combined action of wind speed and direction based on statistical analysis of wind monitoring data at the site of the RSB. The joint probability distribution model is further used to estimate the extreme wind velocity at the deck level of the RSB. The results of the analysis reveal that the probability density function of the maximum entropy method achieves a result that fits well with the monitoring data. Hypothesis testing shows that the distributions of the wind velocity data collected during the past three years do not obey the Gumbel distribution. Finally, our comparison shows that the wind predictions of the maximum entropy method are higher than that of the Gumbel distribution, but much lower than the design wind speed.

Key words: Extreme wind velocity, Maximum entropy theory, Probability density function, Structural health monitoring (SHM)
doi:10.1631/jzus.A1000446 **Document code:** A **CLC number:** U448.25

1 Introduction

During the lifetime of a bridge the mean wind velocity is one of the most important requirements for evaluating the wind resistance of the bridge. Usually the mean wind velocity is statistically described by a random variable model. We have been particularly interested in determining the extreme velocity in a given return period using statistical extrapolation. A lot of effort has been put into estimation of the extreme velocity. Various probability distribution models have been used or proposed for the statistical analysis of recorded wind velocities (Simiu, 1981; Ge and Xiang, 2002; An and Pandey, 2005; Xiao *et al*., 2006). The distributions most commonly used are the extreme value distributions called the Gumbel distribution, the Frechet distribution, and the Weibull distribution (Gumbel, 1958; Mayne, 1979; Simiu and Scanlan, 1996). For example, Ge and Xiang (2002) predicted extreme wind velocities using these three distributions for the Yangpu Bridge in the Shanghai area, and Xiao *et al*. (2006) evaluated the capacity of the Gumbel and Weibull distributions for fitting the extreme wind speed in the Hong Kong area. After the 1970s, most researchers have deemed that the Gumbel distribution is suitable for fitting extreme wind velocity data (Simiu and Scanlan, 1996; Holmes, 2001; Li and Li, 2001; Cook, 2004). As a result, the Gumbel distribution is the method most commonly adopted by structural design codes and standards throughout the world.

Note that during most of the past studies on extreme wind velocity, researchers could only use wind data recorded by meteorological stations located usually far from the sites of the bridges concerned (Ge

‡ Corresponding author

* Project supported by the National Natural Science Foundation of China (Nos. 50725828 and 50808041), the Scientific Research Foundation of Graduate School of Southeast University (No. YBJJ0923), and the Teaching and Research Foundation for Excellent Young Teacher of Southeast University, China

and Xiang, 2002). In the ideal case, there is enough wind data from the bridge site for wind-resistant design and the evaluation of wind resistance during the lifetime of the bridge. In the past decade a significant research effort has focused on the development of structural health monitoring (SHM) for long-span bridges (Ko and Ni, 2005; Deng *et al*., 2010). This has brought new opportunities for researchers who are interested in the wind characteristics and the wind-induced response of bridge structures (Xu *et al*., 2000; Zhu *et al*., 2003; Deng *et al*., 2009; Wang *et al*., 2010). As for the wind-resistant design of long-span bridges, the effect of mean wind velocity on structures is related to not only wind speed but also wind direction. Hence, it is valuable to study the joint distribution of wind speed and its direction using the wind data at the site of the bridge. Until now, little effort has been put into the estimation of the joint distribution and the prediction of the extreme wind velocity using the wind data recorded by the SHM system. The most important reason is that because of the short operation time of most SHM systems, the quantity of recorded wind velocity data may be insufficient when extreme value distributions are used to estimate the extreme wind velocity of the bridges.

Hence, it is necessary to develop a new method to estimate the joint distribution model of wind speed and wind direction from a small sample measured by the SHM system of a bridge. An alternative approach for distribution fitting comes from modern information theory. The maximum entropy theory has been developed as a quantitative approach for seeking a probability distribution, among all possible distributions, that contains a minimum of spurious information (Pandey, 2000; Chen *et al*., 2001).

This paper describes a new joint distribution model of wind speed and direction based on the maximum entropy theory. A relatively small wind velocity sample, collected by the SHM system of the Runyang Suspension Bridge (RSB), China is used to estimate the joint distribution model. The results of the wind velocity sample are compared with the results predicted from the method presented in this paper and those from the Gumbel distribution. The extreme wind velocity in a 100 year return period is then been predicted. Finally, special attention is paid to a comparison between the estimated extreme wind speed and the design wind speed.

2 Basic theory of the maximum entropy method

Shannon (1949) defined a measure of uncertainty, referred to as entropy. Shannon's entropy for a random event is defined as the mathematical expectation of the self-information:

$$S(x)=-\sum_{k=1}^{n}P_k(x)\ln P_k(x), \tag{1}$$

where $P_k(x)$ is the probability of a random variable being equal to x_k. Entropy is a positive, permutationally symmetric quantity which vanishes for a completely certain outcome, and is the maximum when all outcomes are equi-probable. The axiomatic characterization of entropy and its other mathematical properties are given by Kapur and Kesavan (1992). For a continuous variable, x, with the density function $f(x)$, the entropy is expressed as

$$S[f(x)]=-\int_R f(x)\ln[f(x)]\mathrm{d}x, \tag{2}$$

where $S[f(x)]$ is the entropy with the probability density function $f(x)$.

For a discrete random variable, it is

$$S[f(x_i)]=-\sum_{i=1}^{n}f(x_i)\ln[f(x_i)]. \tag{3}$$

Jaynes (1957) presented the maximum entropy principle as a rational approach for choosing a consistent probability distribution, amongst all possible distributions, that contains a minimum of spurious information. The principle of the maximum entropy theory states that the most unbiased estimate of a probability distribution is that which maximizes the entropy subject to constraints supplied by the available information, e.g., the moments of a random variable. The distribution so obtained is referred to as the most unbiased, because its derivation involves a systematic maximization of uncertainty about the unknown information. The mathematical model of the maximum entropy theory is defined as

$$\mathrm{MAX}\ S=-\int_R f(x)\ln[f(x)]\mathrm{d}x, \tag{4}$$

$$\text{ST} \int_R x^i f(x)\mathrm{d}x = m_i,\ i=0, 1, \ldots, N, \tag{5}$$

where m_i is the ith order origin moment from the measured wind speed sample. N is the highest order of m_i. MAX means that when the entropy reaches the maximum, we obtain the best probability density function. ST means that when the equations are satisfied, the entropy will reach the maximum value through the adjustment of the probability density function. To account for the constraints of Eq. (5), the entropy function is expressed as

$$\begin{aligned}\overline{S} = S + (\lambda_0 + 1)\left[\int_R f(x)\mathrm{d}x - m_0\right] \\ + \sum_{i=1}^{N} \lambda_i \left[\int_R x^i f(x)\mathrm{d}x - m_i\right],\end{aligned} \tag{6}$$

where λ_i denotes an unknown Lagrangian multiplier. To derive the function, the entropy is maximized using the usual condition:

$$\frac{\partial \overline{S}}{\partial f(x)} = 0. \tag{7}$$

Let Eq. (6) substitute into Eq. (7) to lead to the following expression of the proper probability density function:

$$f(x) = \exp\left(\lambda_0 + \sum_{i=1}^{N} \lambda_i x^i\right), \tag{8}$$

where N is the highest moment order of the sample. The Lagrangian multipliers are determined by solving a system of nonlinear equations, Eq. (5) to Eq. (8), by a nonlinear least square method that uses a Gauss-Newton optimization algorithm (Chen, 2008). During the calculation process, solving the system of nonlinear equations is converted to a minimum optimization problem. The optimization target function is defined as

$$T(x) = \sum_{i=0}^{N}\left[\int_R x^i f(x)\mathrm{d}x - m_i\right]^2. \tag{9}$$

It is obvious that the function of $f(x)$, among all the probable density functions with the given constraint conditions, which makes the function of $T(x)$ approximate to zero, is the best probability density function. The convergence process of the entropy to the maximum value will be demonstrated in Section 4.3.

3 Statistical analysis of wind monitoring data

3.1 Long-term wind monitoring of the RSB

The subject of this study is the RSB shown in Fig. 1, which is a single-span steel suspension bridge that crosses the Yangtse River, along the highway between Zhenjiang and Yangzhou in China.

Fig. 1 View of the Runyang Suspension Bridge

The main span of the bridge is 1490 m long, making it the longest of its kind in China and the third longest in the world. The SHM system of the RSB has been established to monitor in real time the responses of the bridge under various kinds of environmental actions and mobile loads by the application of modern techniques in sensing, testing, computing and network communication (Li *et al*., 2003). As for the wind environmental monitoring of the bridge, two WA15 anemometers (Fig. 2) produced by the Vaisala Company were installed in the SHM system. One is on the top of the downstream side of the south tower (218.905 m high above the ground), and the other is in the middle of the upstream side of the bridge girder (69.300 m high above the ground).

The anemometers work all day with a working temperature range of from −50 °C–+55 °C and a sampling frequency of 1 Hz. The anemometers were installed to the north and defined the angle of wind direction with 0º to the north, by clockwise rotation. Since May 1, 2005 the anemometers have shown their

high working stability, good performance in dynamic tracking and reliability for measuring data.

The anemometers record not only the wind data under normal wind conditions, but also capture information during typhoons, such as "Matsa" and "Khanun" in 2005. Typical wind speed and direction time histories recorded during typhoon "Matsa", are shown in Fig. 3. Hence, the collected wind records make it possible to provide the data necessary for establishing a joint probability model between the wind speed and its direction at the site of the RSB.

3.2 Statistical characteristics of the wind monitoring data

The daily maximum values of 10-min average wind speed for each of the eight standard compass directions were calculated from May 2005 to November 2007, resulting in a total of 543 data points from the deck of the RSB (the wind data from the deck was used in this study). Fig. 4 shows the frequency of the largest daily wind speed in each direction. In the directions of E, SE and S, the frequencies were 0.21, 0.19 and 0.18, respectively. The frequencies of the other directions were mostly around 0.1 and that from the N direction was only 0.05. Because the site of the bridge is in the region of a subtropical monsoon climate influenced by the ocean monsoon blowing from the East China Sea from the E and S directions, it is logical that the frequencies of the largest daily wind speeds from the S and E directions were much larger than those from the other directions. Hence, Fig. 4 accurately reflects the wind direction characteristics at the site of the RSB. The statistical characteristics of the daily maximum wind speeds used in this study are listed in Table 1.

The statistical surface of the joint probability density function between the wind speed and direction was calculated. Let t_{ij} be the number of the largest daily wind speeds during the wind speed interval $[U_i, U_{i+1}]$ and wind direction interval $[\theta_i, \theta_{i+1}]$. The probability of the largest daily wind speed during the above intervals was calculated approximately as t_{ij}/T, where T is the length of the sample. Considering some

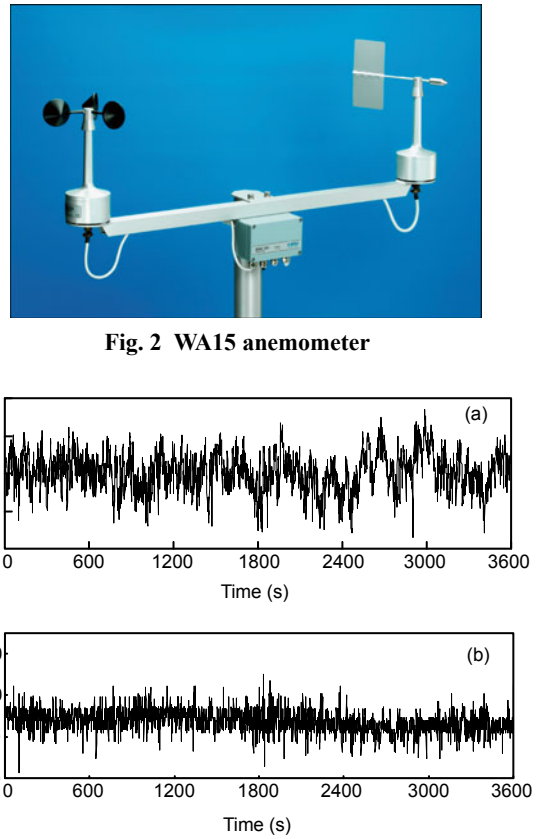

Fig. 3 Typical wind speed (a) and direction (b) time histories on the deck of the RSB during typhoon "Matsa" on August 7 from 3:00–4:00

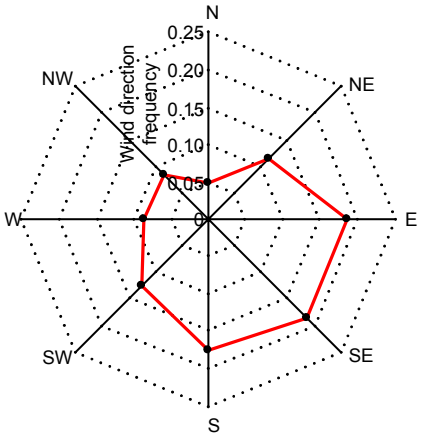

Fig. 4 Wind direction frequency of the largest daily wind speed

Table 1 Statistical characteristics of the daily maximum wind speeds (m/s)

	Daily maximum wind speed								
	N	NE	E	SE	S	SW	W	NW	Non-direction
Mean value μ	6.512	8.771	7.211	7.315	7.241	7.681	8.296	7.479	7.511
Standard deviation σ	2.472	3.262	2.373	2.017	2.177	2.232	2.651	2.961	2.505

necessary expressions, such as $\Delta U_i=U_{i+1}-U_i$, $\Delta\theta_i=\theta_{i+1}-\theta_i$, $\overline{U}_i=(U_{i+1}+U_i)/2$ and $\overline{\theta}_j=(\theta_{j+1}+\theta_j)/2$, the value of the joint probability density at the point of $(\overline{U}_i,\overline{\theta}_j)$ was calculated as

$$P_{ij}=t_{ij}/(T\cdot\Delta U_i\cdot\Delta\theta_j). \tag{10}$$

Using Eq. (10), probability density values of 22×8 points were obtained during the wind speed interval of [0 m/s, 22 m/s] and the wind direction interval of [0°, 360°]. Fig. 5 illustrates the statistical curved surface of the joint probability density function. It can be seen that the maximum values of the probability density were in the wind speed interval of [4 m/s, 10 m/s].

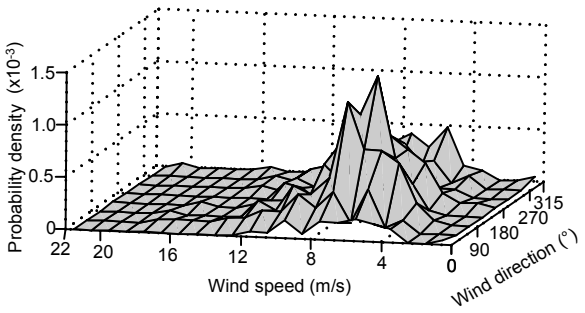

Fig. 5 Statistical curved surface of the joint probability density function

4 Prediction of extreme wind velocity

4.1 Numerical example

Because the highest order of moments in the maximum entropy method usually plays a critical role in the accuracy of the final probability density function, the fitting capacity of the method should be evaluated at first. In this section, the standard normal distribution is employed to compare the fitting capacity of several maximum entropy models. One hundred sets of random numbers obeying a standard normal distribution were generated by the software of MATLAB. The length of each set was 500. The numerical integrations were carried out to determine the exceeding probability. Tables 2 and 3 list the average values of the exceeding probability and reliability indices calculated based on Eqs. (8) and (5), respectively. The reliability index of β, which is related to the exceeding probability, can be defined as

$$\beta=\Phi^{-1}(1-P(x))=-\Phi^{-1}(P(x)), \tag{11}$$

where $\Phi^{-1}()$ denotes the inverse standard normal cumulative distribution function.

In these tables, P_e and β_e are the theoretical values of the exceeding probability and reliability index, respectively, for a given limit value. In Table 2,

Table 2 Results of the exceeding probability

Limit value	P_e	Numerical integrated value			Absolute error		
		3rd-order method	4th-order method	5th-order method	3rd-order method	4th-order method	5th-order method
0	0.500	0.497	0.507	0.507	0.00300	0.00700	0.00700
1	0.158	0.139	0.150	0.145	0.0197	0.00870	0.0134
2	0.0228	0.0141	0.0169	0.0131	0.00869	0.00587	0.00975
3	0.00140	0.000435	0.000605	0.000243	0.000965	0.000795	0.00116
4	3.200×10^{-5}	3.544×10^{-6}	5.844×10^{-6}	6.386×10^{-7}	2.850×10^{-5}	2.620×10^{-5}	3.140×10^{-5}
5	2.910×10^{-7}	6.766×10^{-9}	1.333×10^{-8}	1.623×10^{-10}	2.840×10^{-7}	2.780×10^{-7}	2.910×10^{-7}

Table 3 Results of the reliability indices

Limit value	β_e	Numerical integrated value			Absolute error		
		3rd-order method	4th-order method	5th-order method	3rd-order method	4th-order method	5th-order method
0	0	0.00685	−0.0179	−0.0187	0.00685	0.0179	0.0187
1	1	1.0866	1.0383	1.0570	0.0866	0.0383	0.0570
2	2	2.194	2.122	2.225	0.194	0.122	0.225
3	3	3.329	3.237	3.488	0.329	0.237	0.488
4	4	4.491	4.383	4.843	0.491	0.383	0.843
5	5	5.679	5.562	6.287	0.679	0.562	1.287

the absolute error is the absolute difference between the numerical value of the exceeding probability and P_e. In Table 3, the absolute error is the absolute difference between the numerical value of the reliability index and β_e. The results reveal that the in most cases the absolute errors of the fourth-order moment method are the lowest. This means that the fourth-order moment method has the best accuracy in fitting the approximate probability density function among the three types of maximum entropy methods. Therefore, the fourth-order moment method was used to fit the joint probability density function of the wind speed and its direction.

4.2 Joint probability density functions

It is widely accepted that the effect of wind on structures is related to both the wind speed and its direction. Usually the relationship between the wind speed and its direction is described by a wind rose diagram. For long-span bridges, it is necessary to study the joint action of wind speed and direction on the wind-induced responses of structures. Hence, the joint probability distribution model has been developed to consider the joint effect of wind speed and direction. In this study, based on the probability density function given in Eq. (8), the joint probability density function is defined as

$$f(x)=l(\theta)\exp\left[\lambda_0+\sum_{i=1}^{4}\lambda_i\left(\frac{x-\mu}{\sigma}\right)^i\right]. \tag{12}$$

In Eq. (12), $l(\theta)$ is the wind direction frequency function (Fig. 4). It is obvious that the value of $l(\theta)$ is equal to 1 when the wind direction is not considered. μ is the mean value of the sample, and σ is the standard deviation. $(x-\mu)/\sigma$ is a random variable with a mean value of 0 and a standard deviation of 1. The numerical example of Wei *et al*. (2007) shows that by using Eq. (12) instead of Eq. (8), the convergence speed can be greatly accelerated and the difficulty of convergence failure can be reduced at the same time. In this study, the convergence performance of Eq. (12) was evaluated using the field monitoring data from the following section.

The Gumbel distribution has been the most widely used distribution for fitting extreme wind velocity data (Simiu, 1996; Holmes, 2001; Li and Li, 2001; Cook, 2004). So we compare the fit between the wind velocity data and the results predicted from our proposed method and the Gumbel distribution. The joint function based on the Gumbel distribution is defined as

$$f(x)=l(\theta)\frac{1}{a}\exp\left(-\frac{x-b}{a}\right)\exp\left[-\exp\left(-\frac{x-b}{a}\right)\right], \tag{13}$$

where a and b are the scale parameter and location parameter, respectively.

4.3 Estimation of model parameters

Eq. (12) was adopted rather than the original Eq. (8) because of the advantage of $(x-\mu)/\sigma$ in the convergence. Firstly, without considering the wind direction, a total of 543 sample points were used to evaluate the convergence performance of Eqs. (12) and (8). The highest moment orders of Eqs. (12) and (8) were all four. The convergence processes are demonstrated in Figs. 6 and 7. Note that the iteration step of h in the figures is specifically the iteration step in the Gauss-Newton optimization algorithm. The target function of $T(x)$ has already been defined in Eq. (9). Fig. 6 shows that the iteration step and the target function came to the value of zero after only 23 iterations when Eq. (12) was involved. Fig. 7 shows the convergence process of solving the nonlinear equation system including Eq. (8). The value of the target function in Fig. 7b was still very large after 200 iterations and it seems almost impossible to decrease to zero. So we stopped the solving process. In Fig. 7a, a vertical dotted line divides the curve of iteration step into two phases. In phase I (from about 0−80 times), a slight oscillation in the iteration step is observed. In phase II (from about 80−200), a severe oscillation in the iteration step is observed. The curve in Fig. 7a shows that the more the solving process iterates, the more severe the oscillation of iteration step may be. It can be concluded that Eq. (12) greatly improves the convergence performance of the maximum entropy method compared with the original Eq. (8). Table 4 shows the eight groups of model parameters of the joint probability models for eight compass directions using Eq. (12). The model parameters of Gumbel distributions are shown in Table 5. The model parameters without considering the wind direction are also shown in these tables.

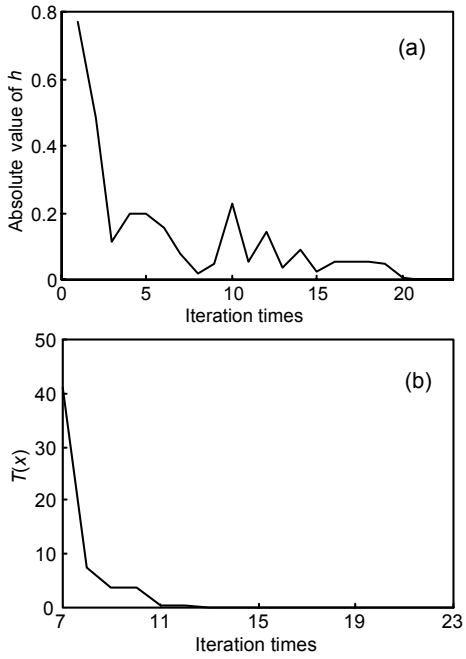

Fig. 6 Convergence process using Eq. (12)
(a) Iteration step of h; (b) Target function of $T(x)$

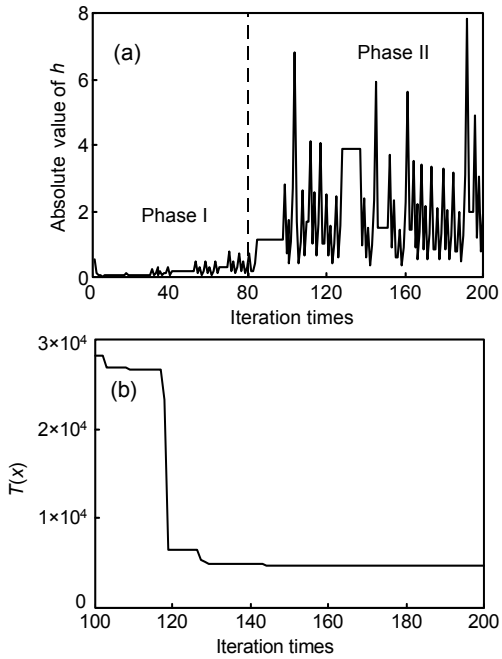

Fig. 7 Convergence process using Eq. (8)
(a) Iteration step of h; (b) Target function of $T(x)$

Table 4 Parameters of the maximum entropy models

Direction	λ_0	λ_1	λ_2	λ_3	λ_4
N	−0.892	0.0125	−0.537	−0.00420	0.00310
NE	−0.960	−0.593	−0.376	0.260	−0.0648
E	−0.838	−0.423	−0.608	0.160	−0.0134
SE	−0.766	−0.741	−0.746	0.326	−0.0383
S	−0.913	−0.0986	−0.504	0.0337	−0.00180
SW	−0.881	−0.630	−0.532	0.268	−0.0444
W	−0.980	−0.0414	−0.351	0.0164	−0.0322
NW	−0.729	−0.580	−0.787	0.247	−0.0208
Non-direction	−0.842	−0.384	−0.602	0.142	−0.0103

Table 5 Parameters of the Gumbel distributions

Direction	Location parameter a	Scale parameter b
N	7.727	2.379
NE	10.484	3.599
E	8.490	3.093
SE	8.441	2.755
S	8.346	2.233
SW	8.874	2.644
W	9.608	2.598
NW	9.167	4.376
Non-direction	8.862	3.306

Fig. 8 compares the fitting results in non-direction from our method with those from the Gumbel distribution. It is clear that the result from the maximum entropy theory gave a much better fit than that of the Gumbel distribution. In Fig. 8 the curve of the Gumbel density function offsets to the higher wind speed, so it is inevitable that the Gumbel distribution model will lead to a lower predicted value. Kolmogorov-Smirnov testing was employed to judge whether the wind speeds obeyed the Gumbel distribution. In this testing of goodness of fit, the total wind speed sample points were assumed to obey the Gumbel distribution with a location parameter of

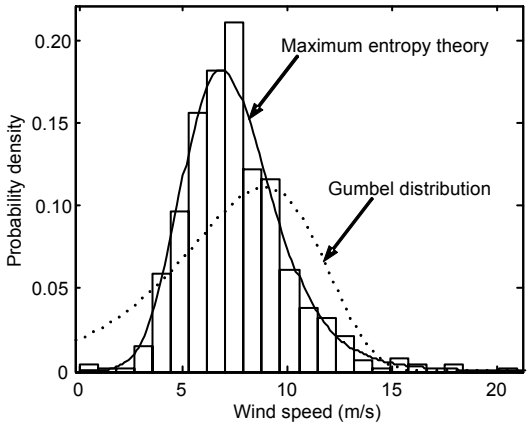

Fig. 8 Fitting results in non-direction

8.862 and a scale parameter of 3.306. The significance level of the testing was set to 0.05. The p value of the testing, that is 2.296×10^{-13}, was far below the significance level of 0.05. So the assumption of the Gumbel distribution was rejected.

Fig. 9 shows the fit between the results from the analytical expression of the probability density function and the histograms of the maximum daily wind speeds. In most wind directions the probability density function coincides with the wind monitoring data.

4.4 Prediction of extreme wind velocity

Based on the above results the expected wind speed U_{100} for the returned period of 100 years in eight compass directions and the non-directional case at the deck level of the RSB can be obtained according to the method stated in the APPENDIX. The predictions of extreme wind velocity are shown in Table 6. For comparison, the predictions of extreme wind velocity have also been calculated using the Gumbel distributions.

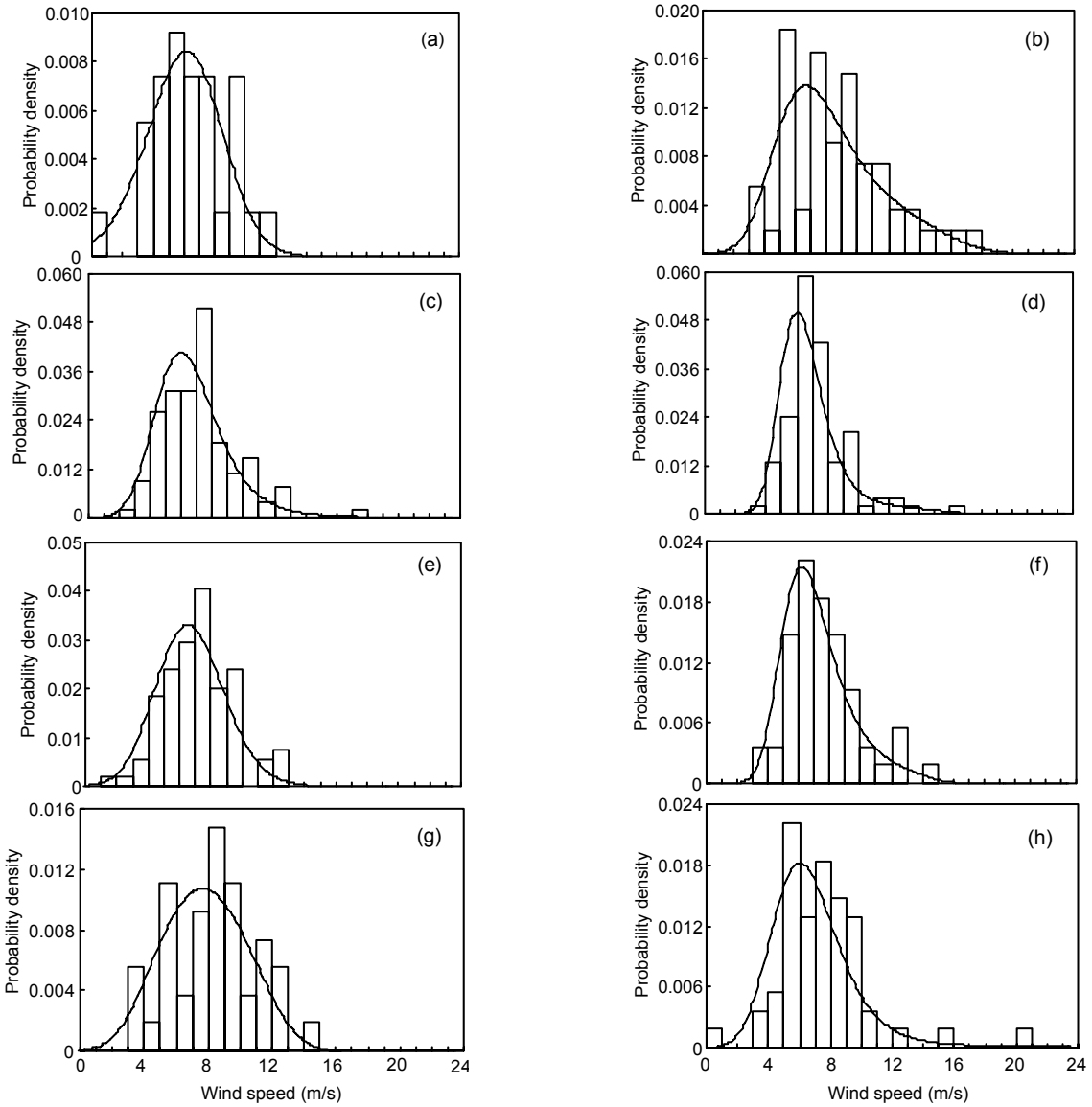

Fig. 9 Fitting results in eight directions

(a) N direction; (b) NE direction; (c) E direction; (d) SE direction; (e) S direction; (f) SW direction; (g) W direction; (h) NW direction

Table 6 Predictions of extreme wind velocity in the return period of 100 years (m/s)

Model type	Wind velocity								
	N	NE	E	SE	S	SW	W	NW	Non-direction
Maximum entropy model	15.7	20.1	22.7	17.6	15.7	16.5	15.8	25.9	24.2
Gumbel distribution mode	12.5	18.1	15.3	14.4	13.2	14.4	15.0	18.4	16.7

The values for the directions of N, SE, S, SW and W were relatively small, but the values for the directions of NE, E, NW and non-direction were larger when calculated using the Gumbel distributions. Hence, the extreme wind speeds vary with the direction and this should be considered in the wind-induced response analysis of the bridge. In addition, the table shows that the extreme wind velocities calculated by the maximum entropy method were larger than those calculated by the Gumbel distribution. The maximum ratio of the value calculated by the maximum entropy theory to the value calculated by the Gumbel distribution was 1.48 in the E direction, and the minimum ratio was 1.05 in the W direction. It can be concluded that the predictions of the extreme wind velocity may be underestimated using the Gumbel distribution model at the site of the RSB.

For the RSB, the design wind speed at a height of 10 m is 29.1 m/s for the return period of 100 years. According to the Wind-Resistant Design Specification for Highway Bridges of China (JTG/T D60-01: 2004), the conversion of the design wind speed at the deck level of the RSB is expressed as

$$U_Z = \left(\frac{Z}{Z_0}\right)^{\alpha} \cdot U_0, \tag{14}$$

where U_0 and U_Z are the design wind speed and the conversion wind speed, respectively. Z is the height at the deck level of the bridge and Z_0 is 10 m. The ground roughness of α is 0.12. So the design wind speed at the deck level U_Z is calculated with the value of 36.7 m/s. It is obvious that the design wind speed is much larger than the predictions of the maximum entropy method. The main reason is that the design wind speed of the RSB is governed usually by typhoon events, while the wind velocity estimation, based on the monitoring data of daily measured wind velocity, is associated with normal wind conditions.

5 Conclusions

This study presents a new method to predict extreme wind velocity based on the maximum entropy theory and its application to the analysis of the wind data measured by the SHM system of the RSB. The following conclusions can be drawn:

1. Wind blowing from the East China Sea from the E and S directions plays a critical role in the wind condition of the site of the RSB. The frequencies of the largest daily wind speed from the S and E directions are much larger than those from other directions, based on the three years of monitoring data.

2. Results of the numerical example show that the fourth-order moment method on the basis of maximum entropy theory has better accuracy in fitting the approximate probability density function than the third-order moment method or the fifth-order moment method.

3. The convergence performance of the maximum entropy method is greatly improved compared with the original method by the normalization of the original variable to a variable with a mean value of 0 and a standard deviation of 1.

4. In non-direction, the fitted curve of the Gumbel density function offsets to the higher value of wind speed and the result of Kolmogorov-Smirnov testing shows that the wind speed sample does not obey the Gumbel distribution. But in most wind directions, results from the density function of maximum entropy method coincide with the wind monitoring data.

5. The extreme wind velocities calculated by the maximum entropy method are larger than those calculated by the Gumbel distribution. Thus, the predictions of the extreme wind velocity may be underestimated using the Gumbel distribution model at the site of the RSB. Finally, the design wind speed is much larger than the predictions of the maximum entropy method.

References

An, Y., Pandey, M.D., 2005. A comparison of method of extreme wind speed estimation. *Journal of Wind Engineering and Industrial Aerodynamics*, **93**(7):535-545. [doi:10.1016/j.jweia.2005.05.003]

Chen, J.H., 2008. The convergence analysis of inexact Gauss-Newton methods for nonlinear problems. *Computational Optimization and Applications*, **40**(1):97-118. [doi:10.1007/s10589-007-9071-7]

Chen, X., Qi, H., Zhang, Y., Wu, C., 2001. Optimal design of a two-stage mounting isolation system by the maximum entropy approach. *Journal of Sound and Vibration*, **243**(4):591-599. [doi:10.1006/jsvi.2000.3230]

Cook, N.J., 2004. Confidence limits for extreme wind speeds in mixed climates. *Journal of Wind Engineering and Industrial Aerodynamics*, **92**(1):41-51. [doi:10.1016/j.jweia.2003.09.037]

Deng, Y., Li, A.Q., Ding, Y.L., Sun, J., 2009. Long-term monitoring and analysis of the wind environment at the site of Runyang Suspension Bridge. *Acta Aerodynamica Sinica*, **27**(6):632-638 (in Chinese).

Deng, Y., Ding, Y.L., Li, A.Q., 2010. Structural condition assessment of long-span suspension bridges using long-term monitoring data. *Earthquake Engineering and Engineering Vibration*, **9**(1):123-131. [doi:10.1007/s11803-010-9024-5]

Ge, Y.J., Xiang, H.F., 2002. Statistical study for mean wind velocity in Shanghai area. *Journal of Wind Engineering and Industrial Aerodynamics*, **90**(12-15):1585-1599. [doi:10.1016/S0167-6105(02)00272-6]

Gumbel, E.J., 1958. Statistics of Extremes. Columbia University Press, NewYork, USA.

Holmes, J.D., 2001. Wind Loading of Structures. Spon Press, London, UK.

Jaynes, E.T., 1957. Information theory and statistical mechanics. *Physical Review*, **106**(4):620-630. [doi:10.1103/PhysRev.106.620]

JTG/T D60-01:2004. Wind-Resistant Design Specification for Highway Bridges. Ministry of Transport, Beijing, China (in Chinese).

Kapur, J.N., Kesavan, H.K., 1992. Entropy Optimization Principles with Applications. Academic Press Inc., San Diego, USA.

Ko, J.M., Ni, Y.Q., 2005. Technology developments in structural health monitoring of large-scale bridges. *Engineering Structures*, **27**(12):1715-1725. [doi:10.1016/j.engstruct.2005.02.021]

Li, A.Q., Miao, C.Q., Li, Z.X., Han, X.L., Wu, S.D., Ji, L., Yang, Y.D., 2003. Health monitoring system for the Runyang Yangtse River Bridge. *Journal of Southeast University (Natural Science Edition)*, **33**(5):544-548 (in Chinese).

Li, G.Q., Li, Q.S., 2001. Theory and Its Application of Time-Dependent Reliability of Engineering Structures. Science Press, Beijing, China (in Chinese).

Mayne, J.R., 1979. The estimation of extreme winds. *Journal of Wind Engineering and Industrial Aerodynamics*, **5**(1-2):109-137. [doi:10.1016/0167-6105(79)90027-8]

Pandey, M.D., 2000. Direct estimation of quantile functions using the maximum entropy principle. *Structural Safety*, **22**(1):61-79. [doi:10.1016/S0167-4730(99)00041-7]

Shannon, C.E., 1949. The Mathematical Theory of Communication. The University of Illinois Press, Urbana, USA.

Simiu, E., 1981. Modern developments in wind engineering: part 1. *Engineering Structures*, **3**(4):233-241. [doi:10.1016/0141-0296(81)90006-7]

Simiu, E., Scanlan, R.H., 1996. Wind Effects on Structures (3rd Ed.). Wiley, NewYork, USA.

Wang, H., Li, A.Q., Jiao, C.K., Li, X.P., 2010. Characteristics of strong winds at the Runyang Suspension Bridge based on field tests from 2005 to 2008. *Journal of Zhejiang University-SCIENCE A (Applied Physics and Engineering)*, **11**(7):465-476. [doi:10.1631/jzus.A0900601]

Wei, Z., Ye, J.H., Shen, S.Z., 2007. Engineering application of the maximum entropy reliability theory. *Journal of Vibration and Shock*, **26**(6):146-152 (in Chinese).

Xiao, Y.Q., Li, Q.S., Li, Z.N., Chow, Y.W., Li, G.Q., 2006. Probability distributions of extreme wind speed and its occurrence interval. *Engineering Structures*, **28**(8):1173-1181. [doi:10.1016/j.engstruct.2006.01.001]

Xu, Y.L., Zhu, L.D., Wong, K.Y., Chan, K.W.Y., 2000. Field measurement results of Tsing Ma Suspension Bridge during Typhoon Victor. *Structural Engineering and Mechanics*, **10**(6):545-559.

Zhu, L.D., Xu, Y.L., Zhang, F., Xiang, H.F., 2003. Measurement of aerodynamic coefficients of tower components of Tsing Ma Bridge under yaw winds. *Wind and Structures*, **6**(1):53-70.

Appendix

Estimation of the extreme wind velocity $U_{\max}$ in the return period of T_0 years.

If the joint probability density function $f(U, \theta)$ has been obtained according to n_0 wind velocity sample points every year, the times of sample appearance in the wind direction interval of $[\theta_j, \theta_{j+1}]$ can be calculated as follows:

$$N_j = T_0 n_0 \int_{\theta_j}^{\theta_{j+1}} \mathrm{d}\theta \int_0^{\infty} f(U,\theta)\mathrm{d}U, \qquad \text{(A1)}$$

where T_0 and n_0 are the return period and wind velocity sample points per year, respectively. In this work T_0 is 100. It should be noted that n_0 is 365 in this work because the largest wind speed point is chosen every day. If the largest wind speed point is chosen every month n_0 should be 12. $f(U, \theta)$ is the joint probability density function of wind speed and wind

direction. In addition N_j is the times of the wind speed sample points in the wind direction interval of $[\theta_j, \theta_{j+1}]$.

During this wind direction interval, the guaranteed rate which the extreme wind velocity has not exceeded can be expressed as

$$P=(1-1/N_j)\int_{\theta_j}^{\theta_{j+1}}\mathrm{d}\theta\int_0^{\infty}f(U,\theta)\mathrm{d}U, \tag{A2}$$

where P is the guaranteed rate.

Substituting Eq. (A1) into Eq. (A2), the guarantee rate P can be expressed as

$$P=\int_{\theta_j}^{\theta_{j+1}}\mathrm{d}\theta\int_0^{\infty}f(U,\theta)\mathrm{d}U-\frac{1}{T_0n_0}. \tag{A3}$$

Meanwhile, the guaranteed rate P also equals the volume enclosed by the curved surface of the joint probability function $f(U, \theta)$ and the rectangular region $0\le U\le U_{\max}$, $\theta_j\le\theta\le\theta_{j+1}$, which can be expressed as

$$P=\int_{\theta_j}^{\theta_{j+1}}\mathrm{d}\theta\int_0^{U_{\max}}f(U,\theta)\mathrm{d}U. \tag{A4}$$

Combining Eq. (A3) with Eq. (A4), the following equation can be obtained:

$$\int_{\theta_j}^{\theta_{j+1}}\mathrm{d}\theta\int_{U_{\max}}^{\infty}f(U,\theta)\mathrm{d}U=\frac{1}{T_0n_0}. \tag{A5}$$

According to Eq. (A5), the extreme wind velocity $U_{\max}$ with the return period T_0 years for all directions can be obtained.